Heat Transfer Enhancement by Sinusoidal-Shaped Disk Rotating in a Forced Flow

Ahmer MEHMOOD[1], Muhammad USMAN[1] , Bernhard WEIGAND[2]

[1]Department of Mathematics & Statistics, FBAS, International Islamic University, Islamabad 44000, Pakistan

[2]Institute of Aerospace Thermodynamics, University of Stuttgart, Germany.

Abstract: *The geometric characteristics of the heat transferring surface and the outer flow conditions have a significant impact on heat transfer augmentation. Both, the surface roughness and the pressure gradient attribute to an enhanced heat transfer. These two effects are utilized in this study to enhance the convective heat transfer rate in a non-similar boundary-layer flow induced by the rotation of a sinusoidal-shaped disk in an external forced flow. The heat transfer coefficient is calculated numerically for the laminar boundary-layer flow with the help of the Keller-box method. The numerical solution of the governing system of equations is first validated by previous published (theoretical and experimental) results for a wavy rotating disk in the absence of an external flow field and also for a flat disk rotating in a forced flow. It is observed that the effect of surface waviness along with a relative fluid motion on heat transfer rate, shear stresses, and shaft torque is quite pronounced. Specifically, enhancement of moment coefficient due to waviness of the disk leads to increase the power of a wavy disk pump in comparison to a smooth one. Furthermore, 119%, 174%, 86%, and 86% enhancement in the heat transfer rate, the radial shear stress, the tangential shear stress, and the moment coefficient, respectively, is observed for a rotating wavy disk subjected to a forced flow (at fixed* $a/\omega = \infty$ *and* $a_0/\lambda = 0.125$*) in comparison to a free rotating flat disk.*

Keywords*: Sinusoidal rotating disk, boundary-layer flow, forced flow, heat transfer enhancement*

Introduction

Numerous industrial applications (turbomachinery, aerospace engineering, flywheels, gear wheels, power engineering, air-cooled turbine disks, gas turbine engines, etc.) have highlighted the requirement of a better understanding of flow and heat transfer in disk pumps. Particularly, there exists a gap for the improvement of the heat transfer process along with the shear stresses on a rotating disk for the prediction of power losses and cooling phenomena in the devices which operate under high speed and high temperatures. The design of the disk texture is essential in acquiring an increased power, efficient pumping capacity and enhanced heat transfer rate in rotating disk systems. Le Palec [1] and Le Palec et al. [2] investigated the role of surface roughness of a rotating disk on the process of heat exchange from the disk surface to the surrounding fluid. They [1, 2] designed a surface roughness with sinusoids which are in fact concentric patterns with respect to the rotation axis, as shown in Fig. 1. The construction of sinusoids on the rotating disk surface yields a significant heat transfer enhancement in comparison to a flat disk. Specifically, selection of an amplitude-to-wavelength ratio (a_0/λ) of the sinusoid equal to 0.2 results in 15% heat transfer augmentation compared to a flat disk as reported by Le Palec [1]. He also confirmed his results by experiments in [2]. However, in the studies

[1, 2], the impact of the surface texture has been analyzed solely in view of the heat transfer. Thus, information of the flow field is missing which has been addressed in detail by Yoon et al. [3]. They discussed the effect of waviness on the torque coefficient and skin-friction coefficient.

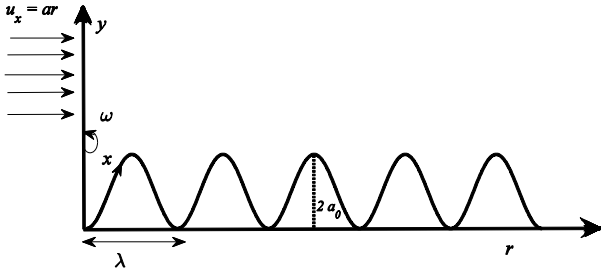

Fig. 1: Schematic of the disk geometry and the used coordinate system.

Interestingly, the limiting case of the above studies [1-3] is the classical von Kármán [4] problem, i.e. the flow over a flat rotating disk which admits a fully self-similar three-dimensional solution and constitutes the basis for most of the three-dimensional flows like flow over a swept wing, aircraft engines, food stuffs in centrifugal pumps, computer disk drivers, flow of waxy crude oil, car brake systems, electrochemistry, etc. Regarding to the importance of this flow, various other related flow characteristics associated with the rotating disk boundary-layer were investigated by several other researchers [5-8] who contributed to this topic in various manners.

Different options can be adopted in consideration of free disk flows depending on whether the ambient fluid is stationary and the disk is rotating or whether the disk is rotating in the presence of an external forced flow or the rotating fluid surrounding the stationary disk etc. These different choices reflect the significant variation in the flow characteristics, which in turn influences the heat transfer rate and other parameters of engineering interest. The external forced flow associated with a rotating smooth disk has been the subject of several studies [9-14] and this class of flow is also considered as a more general problem, having the free rotating disk flow as a limiting case. The relative motion of the disk and the fluid causes a considerable influence on the power needed to spin the flat disk as the torque coefficient increases significantly. Based on these observation Mabuchi et al. [10, 11] studied the effect of external forced flow on heat transfer from a rotating disk, both theoretically and experimentally in the presence of suction/injection. Moreover, an interesting study on the cooling of a rotating disk through forced impingement flow was reported by Shevchuk [14].

A large number of engineering applications require the study of the heat transfer and fluid flow characteristics of a simultaneous forced flow combined with rotation of solid bodies. By combining the useful effects of relative fluid motion along with altered geometrical configurations of the disk surface, as specified by Le Palec [1], it is of practical interest to investigate the flow and heat transfer phenomena in case of relative motion of a wavy disk and a superimposed forced flow (i.e. to predict the heat transfer rate and shear stresses in the situation of relative motion of fluid and sinusoidal-shaped disk). It is worth mentioning that the flows addressed by von Kármán [4], Mabuchi et al. [10], and Le Palec [1] are limiting cases of the current study. The influence of the surface texture of a disk rotating in a superimposed forced flow (refer to Fig. 1) on the heat transfer and the torque coefficients, which are of particular interest in technological applications, is investigated in the present study by numerical calcultions.

Theoretical analysis

Physical model and basic equations

The investigated wavy disk surface is depicted in Fig. 1 along with the associated boundary-layer coordinate system. The coordinate used to measure the radial distance on the wavy disk surface is denoted by x. The normal direction to the disk surface is denoted by y, and the angular variation is measured by θ. A sinusoidal-shaped disk is considered which is rotating in an external flow with a fixed rotation rate ω. The disk surface is specified by a continuous differentiable function, defined by $s(\bar{r}) = a_0 \cos(2N\pi\bar{r})$. The surface roughness, given by the ratio of amplitude-to-wavelength a_0/λ, is an important parameter to signify the role of disk texture on the flow and heat transfer. The role of this ratio is very crucial regarding the development of the boundary-layer. Sufficiently large values of this parameter ($a_0/\lambda > 1$, say) correspond to the situations involving the surface undulations of sufficient height with small wavelength; even smaller than the boundary-layer thickness. Such a situation harms the application of boundary-layer approximation to the governing Navier-Stokes equations. To avoid such a deadlock situation the ratio a_0/λ is assumed here to take values $a_0/\lambda \ll 1$ so that the surface wavelength should remain sufficiently larger than the boundary-layer thickness. Such a favorable assumption ($a_0/\lambda \ll 1$) also ensures the absence of flow separation in the valleys of the wavy surface. As depicted in Fig. 1, the rotating wavy disk is also assumed to be subjected to an external forced flow of the form $u_x(r,\infty) = ar$. The consideration of such an external forced flow restricts the theoretical analysis to certain circumstances. Among which the relationship of the parameter a with the axially incoming velocity u_y and the radial extension of the disk are of fundamental nature. Detailed theoretical and experimental investigation reported by Mabuchi et al. [10-11] and later by Shevchuk [12] resulted in a satisfactory resolve of the above mentioned issues of fundamental nature. Mabuchi et al. [10-11] developed a relationship between the stagnation flow parameter a and the axially incoming velocity u_y of the form $\frac{2u_{y,\infty}}{\pi b}$. They also determined that the edge (at the rim) of the disk affects the flow significantly due to which the flow separation occurs quite interior to the disk rim. They determined that for a finite rotating flat disk their theoretical results were applicable till $r < 0.8b$. Although such a range of radial extension on the disk surface for which theoretical analysis is applicable is not available for wavy disk. But from the results of flat rotating disk we conclude that current analysis concerning a wavy disk does also face similar restriction. For a finite wavy disk the current analysis is applicable till quite inside the disk rim or the disk may be regarded as having an infinite radius otherwise, in order to avoid the edge effects. The disk surface is assumed to be heated with a constant heat flux throughout the disk surface. Far away from the disk surface the fluid assumes the ambient temperature, denoted by T_∞. These boundary conditions can be stated mathematically as

$$\left.\begin{aligned} &u_x = u_y = u_\theta - \omega r = 0, \quad -k\frac{\partial T}{\partial y} = q, \qquad \text{at } y = 0 \\ &u_x = ar, \;\; u_\theta = 0, \;\; T = T_\infty, \qquad\qquad \text{at } y \to \infty \end{aligned}\right\}, \tag{1}$$

where $a\left(=\frac{2u_{y,\infty}}{\pi b}\right)$ is a stagnation flow parameter having the same dimensions as ω. Similarly, the laws of conservation of mass, momentum and energy in view of the above assumptions and by using the boundary-layer assumptions read [15]

$$\frac{\partial u_x}{\partial x} + \frac{\partial u_y}{\partial y} + \frac{u_x}{r}\frac{dr}{dx} = 0, \tag{2}$$

$$u_x\frac{\partial u_x}{\partial x} + u_y\frac{\partial u_x}{\partial y} - \frac{u_\theta^2}{r}\frac{dr}{dx} = \left(u_x\frac{\partial u_x}{\partial x}\right)_{y\to\infty} + \nu\,\frac{\partial^2 u_x}{\partial y^2}, \tag{3}$$

$$u_x \frac{\partial u_\theta}{\partial x} + u_y \frac{\partial u_\theta}{\partial y} - \frac{u_x u_\theta}{r}\frac{dr}{dx} = \nu \frac{\partial^2 u_\theta}{\partial y^2}, \quad (4)$$

$$u_x \frac{\partial T}{\partial x} + u_y \frac{\partial T}{\partial y} = \alpha \frac{\partial^2 T}{\partial y^2}. \quad (5)$$

Here we assumed constant fluid properties and an incompressible, laminar flow. The presence of an external forced flow gives rise to a pressure variation within the boundary-layer which is determined by Bernoulli's equation. However, the pressure variation across the boundary-layer is still negligible.

Normalization

The normalization of the variables has been carried out in the same manner as it was initially done by Le Palec [1]. However, a little modification is still required as the disk rotation rate ω has been replaced by the combined rotation rate $\Lambda = (a^2 + \omega^2)^{1/2}$. Therefore, the new independent variables are defined as

$$\epsilon = \frac{x}{\lambda},\ \eta = \sqrt{\frac{\Lambda R}{\nu \varepsilon}}\, y,$$

(6)

whereby the velocity functions have been replaced by their appropriate relations with the stream functions. Therefore, the normalization of the dependent variables is carried out as

$$f(\epsilon,\eta) = \sqrt{\frac{\Lambda R}{\nu\varepsilon}}\frac{\psi(x,y)}{\Lambda r},\ g(\epsilon,\eta) = \sqrt{\frac{\Lambda R}{\nu\varepsilon}}\frac{\phi(x,y)}{\omega r},\ \Theta(\varepsilon,\eta) = \frac{(T-T_\infty)}{q} k \sqrt{\frac{\Lambda R}{\nu\varepsilon}}, \quad (7)$$

where $R = r/\lambda$, and ψ and ϕ denote the stream functions and are related to the velocity components by as

$$u_x = \frac{1}{r}\frac{\partial(\psi r)}{\partial y}, u_y = -\frac{1}{r}\frac{\partial(\psi r)}{\partial x},\ u_\theta = \frac{\partial \phi}{\partial y}.$$

(8)

Utilizing of Eqs. (6) – (8) into Eqs. (2) – (5) yields the following non-similar system of equations:

$$f_{\eta\eta\eta} - \frac{\varepsilon}{R}\frac{dR}{d\varepsilon}\left(f_\eta^2 - \left(\frac{\omega}{\Lambda}\right)^2 g_\eta^2\right) + \left(\frac{1}{2} + \frac{3}{2}\frac{\varepsilon}{R}\frac{dR}{d\varepsilon}\right) f f_{\eta\eta} + \left(\frac{a}{\Lambda}\right)^2 \frac{\varepsilon}{R}\frac{dR}{d\varepsilon} = \varepsilon\left(f_\eta f_{\eta\varepsilon} - f_{\eta\eta} f_\epsilon\right),$$

(9)

$$g_{\eta\eta\eta} - 2\frac{\varepsilon}{R}\frac{dR}{d\varepsilon} f_\eta g_\eta + \left(\frac{1}{2} + \frac{3}{2}\frac{\varepsilon}{R}\frac{dR}{d\varepsilon}\right) f g_{\eta\eta} = \varepsilon\left(f_\eta g_{\eta\varepsilon} - g_{\eta\eta} f_\epsilon\right),$$

(10)

$$\frac{\Theta_{\eta\eta}}{Pr} + \left(\frac{1}{2} + \frac{3}{2}\frac{\varepsilon}{R}\frac{dR}{d\varepsilon}\right) f \Theta_\eta = \varepsilon\left(f_\eta \Theta_\varepsilon - \Theta_\eta f_\epsilon\right).$$

(11)

These equations are still partial differential equations because of the non-similar nature of the flow owing to the wavy disk texture. Instead, if one considers the flat disk case then a_0/λ tends to zero and the above system becomes independent of ε. Consequently the non-similar partial differential equations reduce to a self-similar form. As the values of a_0/λ depart from zero, the flow character turns to be gradually non-similar. Similarly, the flow character also gradually changes from self-similar to non-similar as one continuously starts to depart from the disk center to the periphery by moving in the radial direction. These facts provide us the solid grounds for the utilization of the von Kármán's self-similar solution as the initial solution in our numerical scheme. As in the present case a_0/λ is non-zero therefore the calculation of the term $\frac{\varepsilon}{R}\frac{dR}{d\varepsilon}$ is mandatory before going to the integration the non-similar equations. This can simply be computed from the information of the disk configuration as

$$\frac{dR}{d\varepsilon} = \sqrt{1 + 4\frac{a_0^2\pi^2}{\lambda^2} sin^2 \frac{2N\pi r}{b}}.$$

(12)

The boundary conditions in terms of the new variables read

$$\left.\begin{aligned} f = g = f_\eta = g_\eta - 1 = \Theta_\eta + 1 = 0, \quad & \text{at } \eta = 0 \\ f_\eta = \frac{a}{\Lambda}, \ g_\eta = 0, \ \Theta = 0, \quad & \text{at } \eta = \infty \end{aligned}\right\}.$$

(13)

Numerical solution

The non-similar Eqs. (9) – (11) subject to the boundary conditions (13) have been solved numerically by implementing the Keller-box method [16] to obtain the velocity and temperature profiles. The validity of the present method is first confirmed by acquiring the flat disk results as well as the Le Palec et al. [2] results. A comparison is shown in Table 1 for the case of a flat disk rotating in an external forced flow reported by Mabuchi et al. [10] with the present numerical results. Our numerical calculations show an excellent agreement with the values reported in Mabuchi et al. [10] (refer to Table 1). The present results for the case of a rough rotating disk are also in very good accordance with those reported by Le Palec et al. [2] (see for instance Figs. 11-13). This validates the numerical procedure used here.

Table 1: Comparison of the present numerical calculations with the work of Mabuchi et al. [10].

	$2f_{\eta\eta}(0)$		$-g_{\eta\eta}(0)$	
a/ω	Mabuchi et al. [10]	Present	Mabuchi et al. [10]	Present
0	1.020	1.020	0.6159	0.6159
0.1	1.037	1.037	0.6413	0.6413
0.25	1.124	1.124	0.6991	0.6991
0.5	1.373	1.373	0.8004	0.8004
1	1.871	1.872	0.9334	0.9335
2	2.332	2.333	1.025	1.025
∞	2.624	2.624	1.075	1.075

Velocity profiles

Radial component of velocity

The radial velocity component in dimensionless form is displayed in Fig. 2 for a surface roughness ratio $a_0/\lambda = 0.1$. The impact of the external flow on the wavy disk is similar to the flat disk case and the disk rotation effects become less pronounced as one increases the values of the ratio a/ω. This means that when the radial pressure gradient starts to dominate, the surface irregularities do not contribute too much to assist the flow induced by the disk rotation. This fact can also be understood form Fig. 3 which elucidates that the positive change in surface roughness ratio corresponds to a very slightly enhancement of the radial component of the velocity and do not interrupt the nature of the flow pattern that was exhibited by the smooth disk. Nevertheless, these two figures are still useful in realizing the enhanced convection caused by the surface undulations on the disk surface. This fact can be mad better visible by choosing smaller value of a/ω.

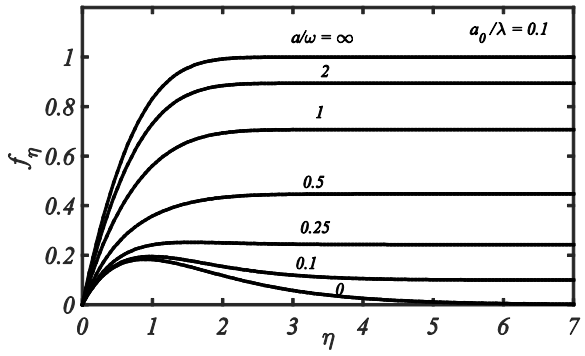

Fig. 2: Variation of the radial velocity component with a/ω for a sinusoidal-shaped disk.

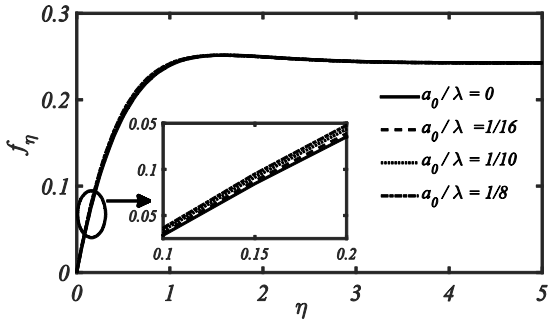

Fig. 3: Variation of the radial velocity component with surface roughness ratio at a fixed $a/\omega = 0.5$.

Circumferential component of velocity

Again the impact of radial pressure gradient on the circumferential velocity component remains the same, as shown in Fig. 4, where the velocity profile shows the typical boundary-layer character. The influence of disk surface texture on this velocity component is also quite weak but it is of the same nature as for the radial component of the velocity shown in Fig. 3. Clearly, the velocity gradient is increased across the boundary-layer which is an indication of the enhanced convective transport (see Fig. 5).

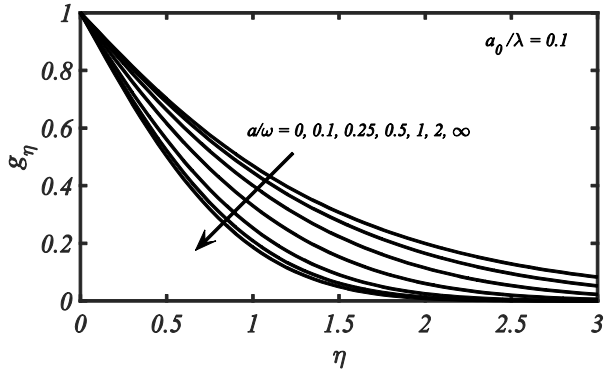

Fig. 4: Variation of the circumferential velocity component with a/ω for a wavy disk.

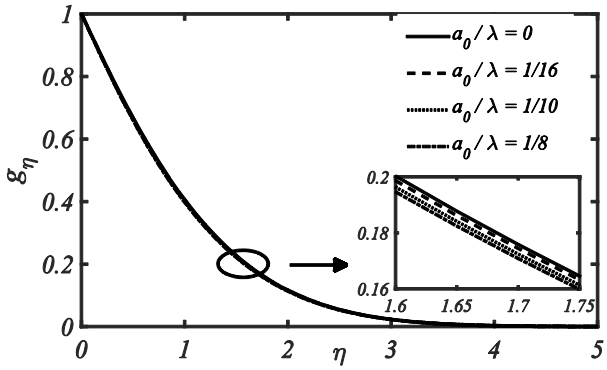

Fig. 5: Variation in circumferential velocity component with surface roughness ratio at a fixed $a/\omega = 0.5$.

Radial and circumferential shear stresses on the wavy disk

The shear stresses acting on the disk surface in radial and circumferential directions due to the radial and azimuthal components of flow are given by

$$\tau_r = \mu \frac{\partial u_x}{\partial y}\Big|_{y=0}, \text{and} \quad \tau_\theta = \mu \frac{\partial u_\theta}{\partial y}\Big|_{y=0}. \tag{14}$$

In terms of dimensionless variables, they are, respectively, transformed into

$$Re_r^{1/2} C_{fr} = 2\sqrt{\frac{R}{\epsilon}}\, f_{\eta\eta}(0,\epsilon), \text{ and } Re_r^{1/2} C_{f\theta} = -2\sqrt{\frac{R}{\epsilon}}\, g_{\eta\eta}(0,\epsilon), \tag{15}$$

where $C_{fr} = \frac{2\tau_r}{\rho r^2 \Lambda^2}$, and $C_{f\theta} = \frac{2\tau_\theta}{\rho r^2 \Lambda^2}$ denote the coefficients of wall skin-friction in the radial and circular directions respectively, and $Re_r = \frac{\Lambda r^2}{\nu}$ represents the local Reynolds number. One can easily recover the relations for a smooth disk from the above ones (Eq. (15)) if one investigates $a_0 \to 0$ (see Mabuchi et al. [10]). The surface roughness ratio (a_0/λ) strongly effects both the local azimuthal and radial skin-friction coefficients, which have been displayed in Figs. 6-7 for a relative motion of the fluid and the disk ($a/\omega = 0.25$). Due to the wavy disk shape, they are also periodic functions but involving a double periodicity in contrast to the surface geometry. This behavior is a consequence of the typical form of the factor $\frac{dR}{d\varepsilon}$ which involves the square of the sinusoidal function. It can also be noticed from Figs. 6-7 that an increase in the amplitude-to-wavelength ratio results in a decrease of these two quantities. Interestingly, both the shear stresses show maximum values for the case of the smooth disk ($a_0/\lambda = 0$) for which the boundary-layer thickness is smallest (see Figs. 2, 4). This suggests that the local shear stresses are smaller in magnitude for the wavy disk in comparison to the smooth disk and it is necessary to calculate the overall shear stresses (by calculating average values) on the whole disk surface in order to see the true picture of the shear stresses generated by the simultaneous rotation and motion of the outer flow. The average values of the radial and tangential shear stresses are obtained by integrating Eq. (15) over the disk surface as

$$\overline{C}_{f\theta} Re_{\mathrm{r}}^{1/2} = \frac{1}{S}\int_S Re_{\mathrm{r}}^{1/2} C_{f\theta}\, dS, \text{ and } \overline{C}_{fr} Re_{\mathrm{r}}^{1/2} = \frac{1}{S}\int_S Re_{\mathrm{r}}^{1/2} C_{fr}\, dS, \tag{16}$$

where S repents the area of the sinusoidal-shaped disk. The influence of surface roughness can be quantified with the help of the area of the smooth disk (πb^2) as a reference, where b is the disk radius. In doing so the corresponding average skin-friction coefficients results in

$$\overline{C}_{f\theta p} = \overline{C}_{f\theta}\frac{S}{\pi b^2}, \text{and} \quad \overline{C}_{frp} = \overline{C}_{fr}\frac{S}{\pi b^2}. \tag{17}$$

These results (Eqs. (16) and (17)) are shown in Figs. 8-9 from where it can clearly be observed that the $\overline{C}_{f\theta}$ and $\overline{C}_{fr}$ both decrease (curves 1 in Figs. 8-9) as the surface roughness ratio a_0/λ increases. But with the contribution of the actual area of the wavy disk the corresponding average shear stresses given in Eq. (17) show higher values in comparison to the smooth disk (refer to curves 2 in Figs. 8-9).

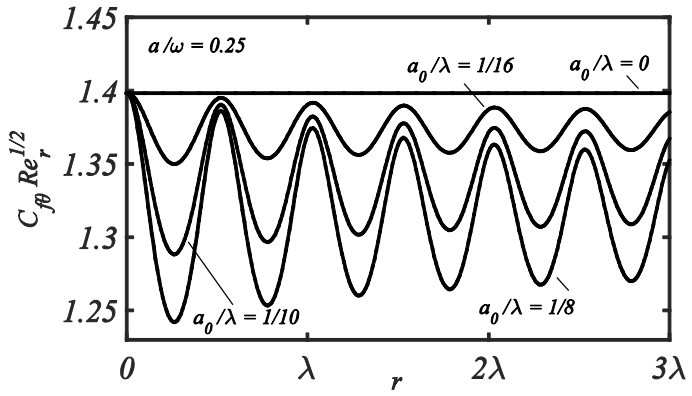

Fig. 6: Local azimuthal skin-friction coefficient as a function of amplitude-to-wavelength ratio with relative motion of disk and fluid.

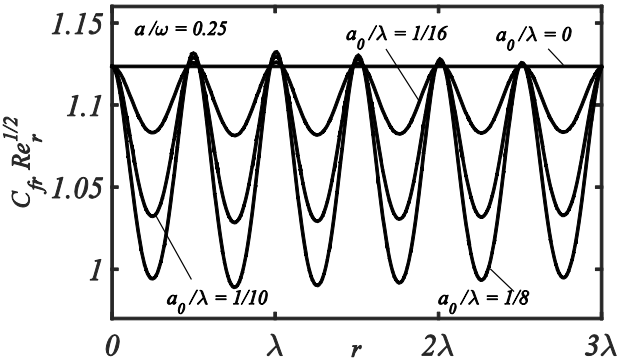

Fig. 7: Local radial skin-friction coefficient as a function of amplitude-to-wavelength ratio with relative motion of disk and fluid.

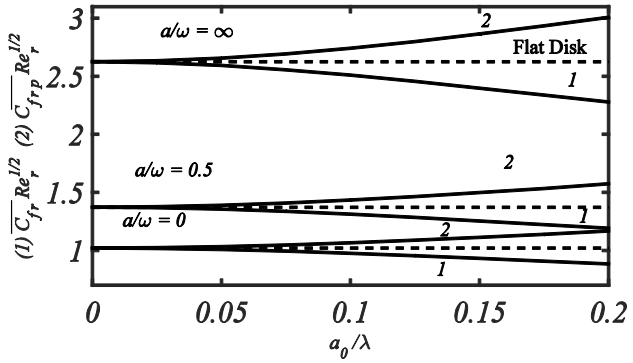

Fig. 8: Influence of amplitude-to-wavelength ratio on average radial skin-friction coefficients $\overline{C}_{fr}$ (curve 1) and $\overline{C}_{frp}$ (curve 2).

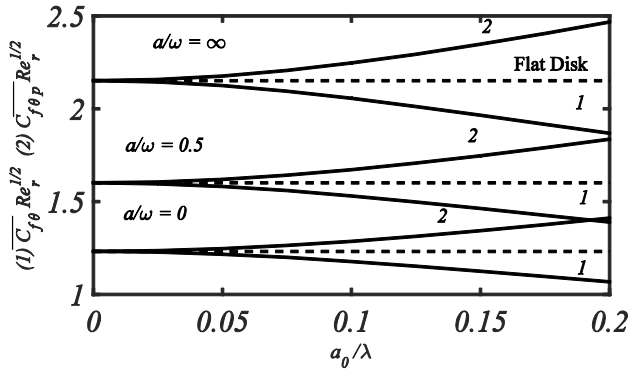

Fig. 9: Influence of amplitude-to-wavelength ratio on average azimuthal skin-friction coefficients $\overline{C}_{f\theta}$ (curve 1) and $\overline{C}_{f\theta p}$ (curve 2).

Both of these shear stresses ($\overline{C}_{f\theta p}$ & $\overline{C}_{frp}$) have been enlarged by up to 15% for a fixed surface roughness ratio (i.e. $a_0/\lambda = 0.2$) due to the wavy surface in the absence of radial pressure gradients. The influence of a relative motion of the disk and the potential flow on these shear stresses can also be seen from these Figs. 8-9. It can be seen that these quantities take higher values due to the increasing radial pressure gradient. Interestingly, in the presence of a radial pressure gradient the wavy surface contributes the same (15%) increment in the shear stresses (refer to Table 2) as it does in the absence of external flow. In comparison to a free rotating flat disk, the radial and tangential shear stresses of the wavy rotating disk in forced flow have been increased up to 174% and 86%, respectively, for fixed $a_0/\lambda = 0.125,\ a/\omega = \infty$.

The influence of the number of sinusoids on the average tangential frictional coefficient ($\overline{C}_{f\theta p}$) is also crucial to be explored. This is presented in Fig. 10 where $\overline{C}_{f\theta p}$ is plotted against the number of waves N fitted to the fixed radius b of the disk. The average tangential shear stress increases slowly when N is varied from 1 to 8. For $N > 4$, its value becomes almost constant.

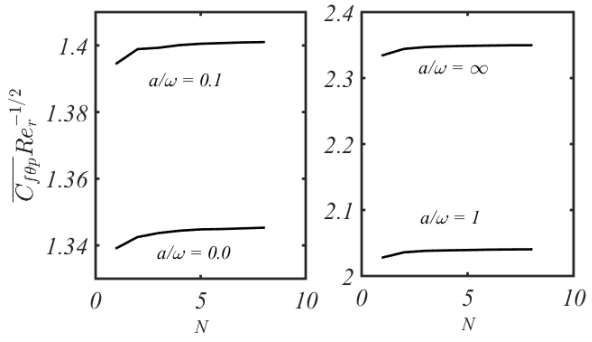

Fig. 10: Dependence of average azimuthal skin-friction coefficient on the number of sinusoids.

Shaft torque of the wavy disk

The total shaft torque (M) of the wavy disk is defined as

$$\bar{M} = -\int r\tau_\theta ds = \int_0^b 2\pi r^2\,\tau_\theta \left(1 + s'^2\right)^{\frac{1}{2}} dr, \tag{18}$$

where the moment coefficient (C_M) is calculated as

$$\overline{C_M} = \frac{4\bar{M}}{\rho\Lambda^2 b^5}. \tag{19}$$

From Table 2, an appreciable increase in torque coefficient is noted for the wavy disk. The disk power is increased up to 7% due to the surface irregularities at $a_0/\lambda = 0.125$ regardless of the absence or presence of the outer potential flow. Although the presence of the external potential flow does increase the disk power but contribution of surface irregularities always stays the same (see Table 2). An increase of 86% in the moment coefficient of the wavy disk is achieved for $a_0/\lambda = 0.125,\ a/\omega = \infty$ in comparison to the free rotating flat disk case (see Table 2).

Table 2: Average azimuthal and radial skin-friction coefficients, moment coefficient, and Nusselt number ($Pr = 0.71,\ N = 3$).

a/ω	a_0/λ	$\overline{C}_{f\theta p}$	$\overline{C}_{frp}$	$\overline{C}_M$	$\overline{Nu}_p$
0	0.0	1.2319	1.0204	1.9351	0.3259
	1/16	1.2543	1.0391	1.9703	0.3318
	1/10	1.2865	1.0656	2.0208	0.3402
	1/8	1.3135	1.0878	2.0633	0.3473
0.1	0.0	1.2827	1.0372	2.0149	0.3587
	1/16	1.3061	1.0562	2.0516	0.3652
	1/10	1.3395	1.0832	2.1041	0.3745
	1/8	1.3677	1.1057	2.1483	0.3823
0.25	0.0	1.3983	1.2325	2.1964	0.4103
	1/16	1.4237	1.1441	2.2363	0.4178
	1/10	1.4602	1.1734	2.2937	0.4285
	1/8	1.4910	1.1978	2.3421	0.4374
0.5	0.0	1.6011	1.3711	2.5150	0.4858
	1/16	1.6300	1.3982	2.5604	0.4946
	1/10	1.6719	1.4340	2.6262	0.5072
	1/8	1.7073	1.4641	2.6819	0.5180
1	0.0	1.8675	1.8720	2.9335	0.5764
	1/16	1.9010	1.9060	2.9862	0.5870
	1/10	1.9498	1.9548	3.0628	0.6020
	1/8	1.9914	1.9961	3.1281	0.6148
2	0.0	2.0512	2.3332	3.2220	0.6368
	1/16	2.0877	2.3752	3.2794	0.6484
	1/10	2.1414	2.4361	3.3637	0.6650
	1/8	2.1869	2.4875	3.4352	0.6790
∞	0.0	2.1505	2.6248	3.3780	0.6690
	1/16	2.1886	2.6718	3.4378	0.6812
	1/10	2.2450	2.7404	3.5264	0.6986
	1/8	2.2927	2.7983	3.6013	0.7133

Heat transfer rate

The calculation of the influence of sinusoidal-shape on the heat transfer on the disk surface is very important. In fact the wavy shape of the disk results in a higher heat transfer rate as anticipated. The local heat transfer rate from the disk surface is computed by looking at the Nusselt number

$$Nu = \frac{h\lambda}{\kappa}, \tag{20}$$

where $h = q_w/(T_w - T_\infty)$ is the local heat transfer coefficient and q_w is the local heat flux at the surface. In view of non-dimensional variables, it is calculated as

$$Re_\Lambda^{-1/2} Nu = \sqrt{\frac{R}{\epsilon}} \frac{1}{\Theta(0)}. \tag{21}$$

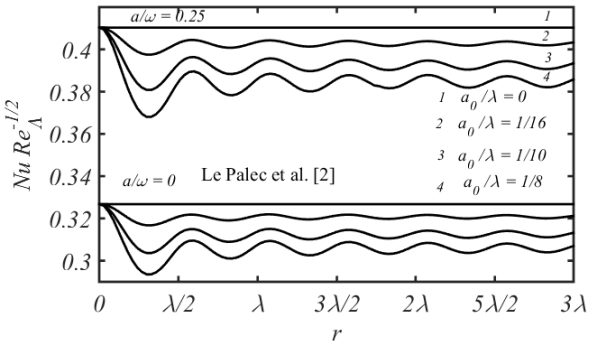

Fig. 11: Local Nusselt number as a function of amplitude-to-wavelength ratio with relative motion of disk and fluid for $Pr = 0.71$.

The effect of surface roughness on local heat transfer coefficient is depicted in Fig. 11 which also shows a double periodicity in the local heat transfer rate with decaying amplitude for the case of $a/\omega = 0$ and 0.25; where an absence of the radial pressure gradient ($a/\omega = 0$) corresponds to the

free rotating wavy disk case investigated by Le Palec et al. [2]. The local heat transfer rate at the wavy disk surface in an external flow is qualitatively the same as for a free rotating wavy disk situation apart from the fact that the relative motion of the disk and fluid is to strengthen the heat exchange from disk to fluid. Similar to the shear stresses, the local heat transfer rates presented in Fig. 11 are lower than the flat disk case and in order to analyze the heat transfer situation, one need to calculate the overall heat exchange from a wavy disk to the surrounding flow, which can be done by computing the average Nusselt number corrected by the surface area ratio. The average Nusselt number relation can be found in a similar manner as the average skin-friction coefficients were calculated and is given by

$$\overline{Nu} Re_{\Lambda}^{-1/2} = \frac{1}{S} \int_S Re_{\Lambda}^{-1/2} Nu \; dS, \tag{22}$$

$$\overline{Nu_p} = \overline{Nu} \frac{S}{\pi b^2}. \tag{23}$$

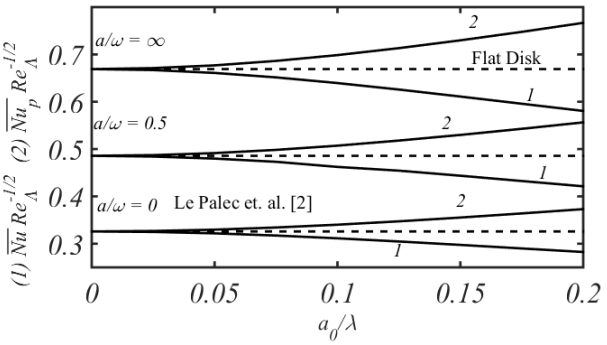

Fig. 12: Influence of amplitude-to-wavelength ratio on average Nusselt number $\overline{Nu}$ (curve 1) and $\overline{Nu_p}$ (curve 2) for $Pr = 0.71$.

The averaged Nusselt number $\overline{Nu_p}$ is shown in Fig.12 from where it can clearly be observed that the $\overline{Nu}$ decreases (curves 1 of Fig. 12) as the ratio a_0/λ increases, while the averaged Nusselt number $\overline{Nu_p}$ (curves 2 of the Fig. 12) increases in comparison to the smooth disk results for increasing values of the surface roughness ratio a_0/λ. In both situations (free rotating disk with and without super imposed forced flow), the overall heat transfer rate is 15% higher due to the shape of the disk (for $a_0/\lambda = 0.2$). The influence of the surface waviness on $\overline{Nu}$ and $\overline{Nu_p}$ in a forced flow is again identical to the case when the disk is rotating freely whereas both the Nusselt numbers ($\overline{Nu}$ and $\overline{Nu_p}$) attained larger values in the presence of an external forced flow. This means that the relative motion of the disk and fluid contribute significantly towards a better cooling of the wavy disk. In Table 2 the enhancement in heat transfer rate due to the waviness and the relative motion of the disk and fluid is reported in detail. In case of $a/\omega = \infty$ and $a_0/\lambda = 0.125$, an enhancement of 119%, in comparison to a free rotating flat disk, has been achieved in heat transfer from the disk to the surrounding fluid. The impact of the number of sinusoids on the average Nusselt number $\overline{Nu_p}$ is finally displayed in Fig. 13. Similar to the results observed for the averaged tangential shear stress only a very small effect of N on $\overline{Nu_p}$ can be observed.

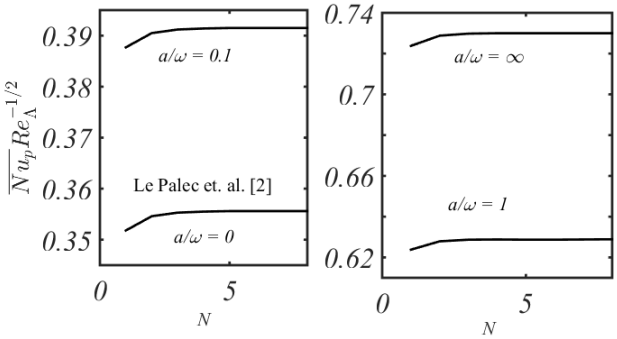

Fig. 13: Dependence of average Nusselt the number on number of sinusoids for $Pr = 0.71$.

Conclusions

A numerical study has been performed for the flow and heat transfer subject to a rotating wavy disk in the presence of forced flow. The numerical solution has been validated for a flat rotating disk case in the presence of an external forced flow with the results reported in [10] and in excellent agreement has been found. Moreover, the authenticity of the present solution is also confirmed with the theoretical and experimental work of Le Palec et al. [2] (i.e. the heat transfer and flow is induced only due to the rotation of sinusoidal-shaped disk) and the present results are in good accordance with those results reported by Le Palec et al. [2]. The present analysis reveals that all physical parameters of interest like the radial and tangential wall shear stresses, moment coefficient, and heat transfer rate (Nusselt number) exhibit a double periodicity in both situations (rotating wavy disk with and without external forced flow) in comparison to the geometrical configuration. Due to the surface roughness almost 15% enhancement in the values of the average radial, azimuthal skin-friction coefficients and the average Nusselt number is observed for both conditions (rotating disk with and without external flow field) for $a_0/\lambda = 0.2$. The moment coefficient is also increased due to the sinusoidal-shape of the disk which in turn shows that the power to spin the disk is increased in comparison to the smooth disk. Furthermore, 119%, 174%, 86%, and 86% enhancement in the heat transfer rate, the radial shear stress, the tangential shear stress, and the moment coefficient is observed for a wavy disk rotating in a forced flow at fixed $a/\omega = \infty$ and $a_0/\lambda = 0.125$ in comparison to a free rotating flat disk. This fact highlights the benefits of a disk with sinusoidal waves under the action of an external forced flow.

Acknowledgements: The first author thanks the Alexander von Humboldt Foundation for the financial sponsorship as the work was initiated during his post-doctoral fellowship period.

References

1. Le Palec, G., Numerical study of convective heat transfer over a rotating rough disk with uniform wall temperature, Int. Com. Heat Mass Tranf. 16 (1989), pp. 107-113.
2. Le Palec, G., Nardin, P., Rondot, D., Study of laminar heat transfer over a sinusoidal-shaped rotating disk, Int. J. Heat Mass Transf. 33 (1990), pp. 1183-1192.
3. Yoon, M. S., Hyun, J. M., Park, J. S., Flow and heat transfer over a rotating disk with surface roughness, Int. J. Heat and Fluid Flow, 28 (2007), pp. 262-267.
4. von Kármán, T., Uber laminare und turbulente Reibung. Z. Angew. Math. Mech. 1 (1921), pp. 233-252.
5. Cochran, W. G., The flow due to a rotating disk, Proc. Cambridge Philos. Soc. 30 (1934), pp. 365-375.
6. Benton, E. R., On the flow due to a rotating disk, J. Fluid Mech., 24 (1966), pp. 781-800.
7. G. Evans, G., Grief, R., A numerical model of the flow and heat transfer in a rotating disk chemical vapor deposition reactor. ASME J. Heat Transf., 109 (1987), pp. 928-935.
8. Rogers, M. H., Lance, G. N., The rotationally symmetric flow of a viscous fluid in the presence of an infinite rotating disk. J. Fluid Mech., 7 (1960), pp. 617-631.
9. Tien, C. L., Tsuji, J., Heat transfer by laminar forced flow against a non-isothermal rotating disk, Int. J. Heat Mass Transf., 7 (1963), pp. 247-252.
10. Mabuchi, I., Tanaka, T., Kumada, M., Studies on convective heat transfer from a rotating disk (3rd Report, Heat and mass transfer in a laminar flow about a rotating disk with suction or injection in the axial stream). Bull JSME, 11 (1968), pp. 875-884.

11. Mabuchi, I., Tanaka, T., Sakakibara, Y., Studies of convective heat transfer from a rotating disk (5th Report, Experiment on the laminar heat transfer from a rotating isothermal disk in a uniform forced stream). Bull JSME, 14 (1971), pp. 581-589.
12. Hannah, D.M., Forced flow against a rotating disc, British Aero. Res. Comm. Rep. and Memo No., 2772 (1947).
13. Tifford, A. N., Chu, S. T., On the flow around a rotating disc in a uniform stream, J. Aero. Sci., 19 (1952), pp. 284-285.
14. Shevchuk, I.V., Laminar heat transfer in a rotating disk under conditions of forced air impingement cooling: approximate analytic solution, Heat and Mass transf. and Physical Dynamics, 5 (2002), pp. 739-747.
15. Moore, F. K., Three-dimensional boundary layer theory, Advances in Applied Mechanics, 4 (1956), pp. 159-228.
16. H.B. Keller, T. Cebeci, Accurate numerical methods for boundary-layer flows-I. Two dimensional laminar flows, Proc. IInd Int. Conference on Numerical Methods in Fluid Dynamics, (1971), pp. 92-100.

Nomenclature

a	pure constant, s^{-1}
a_0	amplitude of wavy disk, m
b	disk radius, m
$C_{fr},\ C_{f\theta}$	r, θ components of local shearing, $-$
$\overline{C_{fr}}, \overline{C_{f\theta}}$	average shear stresses on the disk surface, $-$
$\overline{C_{frp}},\ \overline{C_{f\theta p}}$	average radial and tangential shear stresses related to flat disk surface, $-$
$\overline{C_M}$	moment coefficient, $-$
$f(\varepsilon,\eta), g(\epsilon,\eta)$	dimensionless stream functions, $-$
$\bar{M}$	rotating torque, kg $m^2 s^{-2}$
N	number of sinusoids, $-$
Nu	local Nusselt number, $-$
$\overline{Nu}$	average Nusselt number related to the actual disk surface, $-$
$\overline{Nu_p}$	average Nusselt number related to the flat disk surface, $-$
Pr	Prandtl number, $-$
q_w	uniform wall heat flux, kg s^{-3}
R	dimensionless radial distance, r/λ, $-$
r	radial distance from the rotation axis, m
$\bar{r} = r/b$	dimensionless coordinate, $-$
Re_r	local Reynolds number, $\Lambda r^2/\nu$, $-$
Re_Λ	rotational Reynolds number, $a\Lambda^2/\nu$, $-$
S	actual disk surface area, m^2
T	fluid temperature in the boundary-layer, K
T_∞	ambient temperature, K
u_x, u_θ, u_y	velocity components, m s^{-1}
x	direction along the disk surface, m
y	normal to the surface, m

Greek symbols

α	thermal diffusivity of the fluid, $\mathrm{m^2 s^{-1}}$
δ	boundary-layer thickness, m
ϵ	dimensionless coordinate, x/λ, $-$
η	dimensionless variable, $-$
θ	azimuthal direction, $-$
Θ	dimensionless temperature, $-$
κ	thermal conductivity, kg m $s^{-3}\mathrm{K^{-1}}$
λ	wavelength, m
Λ	combined rotation rate, $\Lambda = (a^2 + \omega^2)^{1/2}$, $\mathrm{s^{-1}}$
μ	dynamic viscosity of the fluid, kg. $(\mathrm{ms})^{-1}$
ν	kinematic viscosity of the fluid, $\mathrm{m^2 s^{-1}}$
τ_r, τ_θ	radial and tangential wall shear stresses, kg $\mathrm{m^{-1}} s^{-2}$
$\psi(x,y), \phi(x,y)$	stream functions, $\mathrm{m^2 s^{-1}}$
ω	rotation rate, $\mathrm{s^{-1}}$